

Original Article

Rapamycin inhibits peritoneal fibrosis by modifying lipid homeostasis in the peritoneum

Jing Liu, Chun-Ming Jiang, Yuan Feng, Wei Zhu, Bo Jin, Yang-Yang Xia, Qing-Yan Zhang, Peng-Fei Xu, Miao Zhang

Institute of Nephrology, Affiliated Drum Tower Hospital, Medical School of Nanjing University, Nanjing 210008, Jiangsu Province, China

Received October 17, 2018; Accepted February 5, 2019; Epub March 15, 2019; Published March 30, 2019

Abstract: Peritoneal fibrosis (PF) is characterized by progressive accumulation of extracellular matrix (ECM) components in the peritoneum under high glucose conditions. Rapamycin has previously been shown to inhibit ECM accumulation of peritoneal mesothelial cells (PMCs) and prevent PF. Here we explored the undefined mechanisms by which rapamycin inhibits ECM accumulation of PMCs. We used high-glucose peritoneal dialysis solution (PDS) in a mouse peritoneal dialysis model to induce *in vivo* PF and in human PMCs *in vitro* to stimulate ECM accumulation. The mice that received chronic PDS infusions showed typical features of PF, including markedly increased peritoneal thickness, excessive matrix deposition, increased peritoneal permeability, and higher expressions of α -smooth muscle actin and collagen I. Rapamycin significantly ameliorated these pathological changes. There was a parallel decrease in lipid accumulation in the peritoneum of rapamycin-treated mice. Rapamycin significantly inhibited high-glucose PDS-induced ECM accumulation and reduced the lipid droplet in human PMCs in the presence of PDS. The effects of rapamycin on intracellular lipid metabolism correlated with a series of steps in lipid homeostasis; namely, a decrease in low density lipoprotein receptor-mediated lipid influx, which was mediated through the downregulation of sterol regulatory element-binding protein-2 (SREBP-2) and SREBP cleavage-activating protein (SCAP), and an increase in adenosine triphosphate-binding cassette transporter A1-mediated lipid efflux, which was mediated through the upregulation of the liver X receptor α and peroxisome proliferator-activated receptor α . We conclude that rapamycin shows a clear protective effect on high-glucose PDS-induced PF by improving the disruption of intracellular lipid homeostasis.

Keywords: Rapamycin, high-glucose peritoneal dialysis solution, peritoneal fibrosis, lipid homeostasis

Introduction

Peritoneal dialysis (PD) is an alternative treatment for end-stage renal disease that uses the peritoneum as a permeable barrier for the exchange of nocuous substances and water [1]. During PD, long-term exposure to high-glucose concentration PD solutions (PDS) causes damage to the peritoneum, which subsequently can lead to increased synthesis of extracellular matrix (ECM) components by peritoneal mesothelial cells (PMCs), leading to submesothelial fibrosis, ultrafiltration failure, and eventual discontinuation of PD [2, 3].

Recent reports suggest that abnormal lipid homeostasis may contribute to the pathogenesis of multiorgan fibrosis, such as renal fibrosis

[4], vascular sclerosis [5], non-alcoholic fatty liver disease [6], and cardiac fibrosis [7]. Interestingly, Chang *et al.* found that lipid-lowering agents (e.g., statins) inhibit ECM accumulation in high-glucose-treated PMCs and PDS-stimulated rats via the mevalonate pathway. In fact, statins exert these effects by preventing the synthesis of other important isoprenoids of the cholesterol biosynthetic pathway, which suggests that disruption of lipid homeostasis may contribute to the pathogenesis of PF caused by high-glucose concentration PDS [8]. In most cells, intracellular lipids are governed by tight regulation of cholesterol influx and efflux pathways [9]. The low-density lipoprotein receptor (LDLr) in the liver is of primary importance for the binding and internalization of plasma-derived LDL cholesterol and in regulating

Rapamycin-induced inhibition of peritoneal fibrosis

intracellular LDL influx. *LDLr* gene expression in mammalian cells is predominantly regulated via a negative-feedback mechanism that depends on mediation of intracellular cholesterol concentrations by sterol regulatory element-binding proteins (SREBPs) and SREBP cleavage-activating protein (SCAP). When cells have sufficient cholesterol, SCAP and SREBP-2 form a complex that is retained in the endoplasmic reticulum (ER), where they remain inactive as transcription factors, resulting in limited intracellular cholesterol by downregulation of *LDLr* [10]. Cholesterol and phospholipid efflux pathways are mediated by cell membrane transporter proteins, such as adenosine triphosphate (ATP)-binding cassette transporter A1 (ABCA1). Liver X receptors (LXRs) and peroxisome proliferator-activated receptors (PPARs) are important nuclear receptors that control the transcription of various specific genes. Studies have suggested that LXRs and PPARs upregulate ABCA1 expression, thereby providing an amplification loop for ABCA1 expression and further decreasing intracellular cholesterol and phospholipids [11].

Rapamycin is a commonly used immunosuppressive agent that inhibits the mammalian target of rapamycin (mTOR) and has been demonstrated to have anti-fibrotic activity in the kidneys [12], liver [13], and cardiovascular system [14], as well as in systemic sclerosis [15]. One of the key actions of rapamycin against fibrosis is inhibition of intracellular lipid accumulation. Our previous work suggests that rapamycin blocks *LDLr*-mediated cholesterol uptake in HepG2 cells and vascular smooth muscle cells (VSMCs) via inhibition of SREBP-2 and decreased SCAP/SREBP-2 complex translocation from the ER to the Golgi apparatus [13, 14]. Conversely, rapamycin increases cholesterol efflux from VSMCs [16], macrophages [17], and glomerular mesangial cells [18] via increased expression of ABCA1. Therefore, rapamycin may contribute to the maintenance of intracellular lipid homeostasis by both reducing cholesterol uptake and increasing cholesterol efflux, ultimately preventing lipid disorder-mediated organ injury. Recent studies report that rapamycin is also effective in suppressing ECM deposition of PMCs and preventing PF under high-glucose conditions in the peritoneum [19, 20]. However, the underlying relation-

ship involved between rapamycin and PF induced by exposure to high-glucose PDS has not been thoroughly elucidated to date.

The present study was undertaken to explore whether rapamycin inhibits lipid accumulation and ECM deposition of PMCs under high-glucose PDS stimulation, in turn improving lipid disorder-mediated PF.

Materials and methods

Ethics statement

This study was carried out in strict accordance with the recommendations of the Guide for the Care and Use of Laboratory Animals of the National Institutes of Health. The protocol was approved by the Committee on the Ethics of Animal Experiments of Nanjing Drum Tower Hospital (Nanjing City, China). All animals were anesthetized with sodium pentobarbital during surgery, and all efforts were made to minimize discomfort.

Animal model

Male C57BL/6 mice purchased from the Model Animal Research Center of Nanjing University were used in this study. Thirty-eight-week-old mice were randomly divided into three groups of 10 mice each. Control mice received a daily intraperitoneal injection of 3 ml phosphate buffered saline (PBS) for 8 weeks, PDS mice received a daily intraperitoneal injection of 3 ml 4.25% glucose PDS (Baxter, 6AB9896) for 8 weeks, and PDS-plus-Rapa mice received daily intragastric administration of 1 mg/kg rapamycin (Selleck Chemicals, s1039) at later time points (weeks 5-8), based on the PD-model group, for a total of 4 weeks. The volume and concentration of PDS and rapamycin used were based on results of previous studies [19, 21]. At termination, peritoneal permeability was tested, and peritoneal tissues (including the parietal peritoneum and visceral peritoneum) were used for histological assessments and western blot analyses.

Peritoneal permeability

Modified peritoneal equilibration tests (PETs) were performed to determine the peritoneal permeability before the mice were sacrificed.

Rapamycin-induced inhibition of peritoneal fibrosis

After intraperitoneal injection of 3 ml 4.25% glucose PDS, dialysate and blood samples were collected at 0 and 2 h of dwell time. Concentrations of glucose and blood urea nitrogen (BUN) in dialysate and plasma were measured in the laboratory of the Clinical Biochemistry Department in Nanjing Drum Tower Hospital. The peritoneal permeability was determined by glucose absorption from dialysate (D/D0) and the dialysate-to-plasma (D/P) ratio of BUN [21].

Histology and immunohistochemistry staining

The parietal peritoneum was fixed with 4% paraformaldehyde and embedded in paraffin. The thickness of the peritoneum was stained with hematoxylin and eosin (H&E), and imaged under light microscopy ($\times 200$). Peritoneum sections were deparaffinized and stained with Masson's trichrome stain for quantification of fibrosis. The results were observed under light microscopy ($\times 200$). For immunohistochemistry staining, deparaffinized sections were placed in citrate-buffered solution (pH 6.0) and heated for antigen retrieval. Endogenous peroxidase was blocked with 3% hydrogen peroxide, and nonspecific antibody binding was blocked with 10% goat serum. Subsequently, sections were incubated with α -smooth muscle actin (α -SMA) (Abcam, ab7817) and collagen I (Santa Cruz, sc-25974) primary antibodies overnight at 4°C followed by incubation with biotinylated secondary antibodies. Finally, a diaminobenzidine tetrahydrochloride substrate was used to initiate the reaction. The results were observed under light microscopy ($\times 200$). Semiquantitative analysis was performed with Image-Pro Plus version 5.0 software.

Observation of lipid accumulation

The lipid accumulation in the parietal peritoneum was evaluated by Oil Red O (ORO) staining and filipin staining. The results of ORO staining were observed under light microscopy ($\times 200$) and the results of filipin staining were examined by laser microscopy ($\times 200$). Semiquantitative analysis was performed with Image-Pro Plus version 5.0 software.

Cell culture

Human PMCs (HPMCs; HmrSV5, Cell Bank of the Chinese Academy of Sciences, Shanghai, China) were cultured with Dulbecco's Modified

Eagle's Medium (DMEM; Gibco, 10567-014) containing 10% fetal bovine serum (Gibco, 16000044). Experiments were stimulated with 4.25% glucose PDS (Baxter, 6AB9896) and rapamycin (Selleck Chemicals, s1039).

Exposure of HPMCs to high-glucose PDS and rapamycin

Sub-confluent HPMCs grown in a culture dish were incubated with serum-free medium for 24 h to arrest and synchronize the cell growth. Next, four groups were defined as follows: group 1, control (HPMCs without any stimulation); group 2, PDS (HPMCs stimulated with 2 ml 4.25% PDS); group 3, Rapa (HPMCs treated only with 10 ng/ml rapamycin); group 4, PDS plus Rapa (HPMCs co-treated with 2 ml 4.25% PDS and 10 ng/ml rapamycin). The observation time points of cultures were every 24 h.

Quantitative measurement of intracellular free cholesterol/cholesterol ester by high-performance liquid chromatography (HPLC)

Briefly, cells were collected and lipids were extracted by adding 1 ml chloroform/methanol (2:1). The lipid phase was collected, dried in a vacuum, and then dissolved in 2-propanol containing 10% Triton X-100. The concentrations of total and free cholesterol in each sample were analyzed using a standard curve normalized against total cell protein. The concentration of cholesterol ester was calculated by subtracting the amount of free cholesterol from the total cholesterol.

Quantification of specific transcripts by real-time polymerase chain reaction (RT-PCR)

Total RNA was isolated from cultured HPMCs using the guanidinium-phenol-chloroform method. Total RNA (500 ng) was used as a template for reverse transcription PCR for cDNA synthesis, performed using a kit from TaKaRa Biotechnology. Resulting cDNA was divided for separate amplification of target genes using specific primers designed by Taqman Primer Express Software V2.0 and shown in **Table 1**. RT-PCR was performed in an ABI 7300 RT-PCR system using a SYBR Green PCR kit according to the manufacturer's protocol (TaKaRa Biotechnology). After RT-PCR, a dissociation curve (melting curve) was constructed for the range of 60-95°C. The relative amount of mRNA was calculated using the comparative threshold

Rapamycin-induced inhibition of peritoneal fibrosis

Table 1. Human TaqMan Primers for Real-time PCR

Genes	Primer sequences
α -SMA	Sense: 5'ACCCACAATGTCCCATCTA3' Antisense: 5'GAAGGAATAGCCACGCTCAG3'
Collagen I	Sense: 5'CTGCAAGAACAGCATTGCAT3' Antisense: 5'GGCGTGATGGCTTATTTGTT3'
LDLr	Sense: 5'GCGAAAGAAACGAGTCCAG3' Antisense: 5'TGACAGACAAGCACGTCTCC3' Sense: 5'ATCGCTCCTCCATCAATGAC3'
SREBP-2	Antisense: 5'TTCCTCAGAACGCCAGACTT3' Sense: 5'TGAGCAGCCTGAGTGGTATG3'
SCAP	Antisense: 5'TGTCTCTCAGCACGTGGTTC3' Sense: 5'GCAGCAGAGCGAGTACTTCGTT3'
ABCA1	Antisense: 5'CAAGACTATGCAGCAATGTTTTTGT3' Sense: 5'AGAAGAACAGATCCGCCTGAAG3'
LXR α	Antisense: 5'GGCAAGGATGTGGCATGAG3' Sense: 5'CGTGCTTCTGCTTCATAGATAAG3'
PPAR α	Antisense: 5'GTGGTAGCGCTGGTCTAC3' Sense: 5'CTACCTCATGAAGATCCTCACCGA3'
β -actin	Antisense: 5'TTCTCCTTAATGTCACGCACGATT3'

cycle ($\Delta\Delta Ct$) method. The amplification efficiencies of the target and reference genes were shown to be approximately equal to the slope of the log input amount to $Ct < 0.1$. Controls consisting of nuclease-free H₂O or RNA samples that were not reverse transcribed were negative for the target and reference genes.

Western blot analysis

Identical amounts of total protein extracts from cultured HPMCs and peritoneums of C57BL/6 mice were denatured and resolved by electrophoresis. The membranes were blocked with blocking buffer for 1 h at room temperature after gel transfer. Membranes were then incubated overnight at 4°C with primary antibodies for LDLr (Santa Cruz, sc-11824), SREBP-2 (Santa Cruz, sc-271615), SCAP (Abcam, ab190103), ABCA1 (Abcam, ab18180), LXR α (Abcam, ab41902), PPAR α (Santa Cruz, sc-398394), α -SMA (Abcam, ab7817), and collagen I (Santa Cruz, sc-25974) followed by horseradish peroxidase-labeled secondary antibodies for 1 h. Finally, the bands were detected using an enhanced chemiluminescence advanced system (Amersham Biosciences, UK).

Statistical analysis

All data are expressed as the mean \pm standard deviation (SD) and were analyzed with SPSS

16.0 software. One-way ANOVA was used to compare continuous variables among groups where appropriate. The correlation analysis was calculated using Spearman's rank correlation. A difference was considered significant if the p -value was < 0.05 .

Results

Rapamycin prevents PF and functional injury in a PD mouse model

After 8 weeks of PD in mice, H&E and Masson's trichrome staining revealed that PDS mice receiving no treatment showed typical features of PF, including thickening of the submesothelial compact zone within the anterior abdominal wall and collagen deposition, compared to normal control mice (**Figure 1A**). These pathological changes were associated with increased peritoneal permeability, determined by peritoneal equilibration tests (**Figure 1B** and **1C**). In contrast, rapamycin prevented peritoneal thickening and collagen deposition as well as peritoneal dysfunction (**Figure 1**). These protective effects against PF were further demonstrated by treatment of rapamycin to inhibit α -SMA and collagen I protein expression levels (**Figure 2A-D**).

Rapamycin prevents lipid accumulation in a PD mouse model

We examined the preventive effect of rapamycin on lipid accumulation in response to chronic high-glucose PDS infusion. Compared to the control, a significant increase in lipid accumulation was observed in the high-glucose PDS-treated peritoneal tissue, demonstrated by ORO and filipin staining. However, rapamycin decreased the high-glucose PDS-stimulated lipid droplet deposition (**Figure 3A**). This finding was consistent with the results from semiquantitative analyses of ORO (**Figure 3B**) and filipin staining (**Figure 3C**).

Relationship between PF and lipid accumulation in a PD mouse model

As shown in **Figure 4**, we performed correlation analyses of lipid deposition using data from the semiquantitative analyses and the protein expression levels of α -SMA and collagen I from western blot analyses. Positive correlations were observed between the data from ORO staining and the protein expression levels of α -SMA ($r = 0.782$, $P = 0.013$) and collagen I ($r =$

Rapamycin-induced inhibition of peritoneal fibrosis

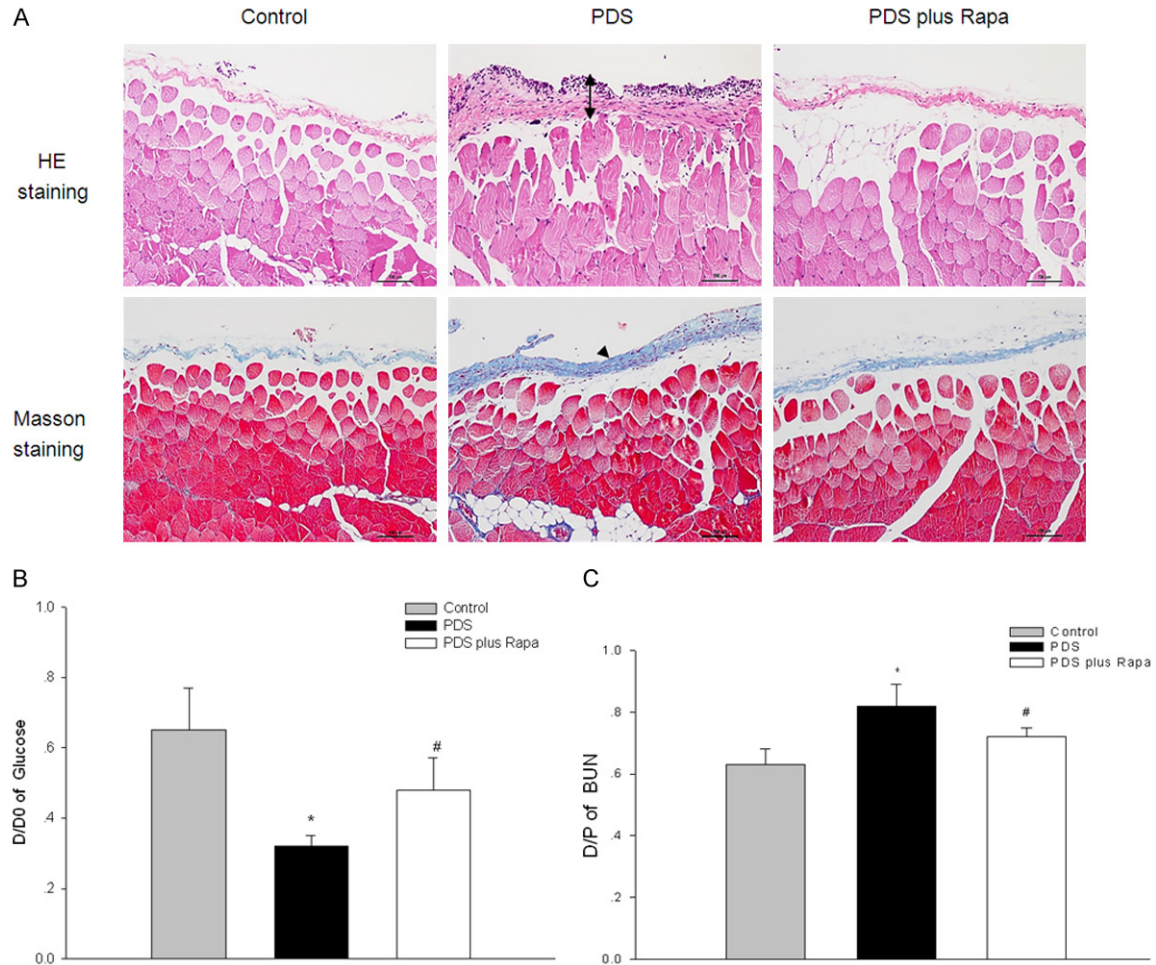


Figure 1. Rapamycin prevented PF and functional injury in a mouse model of PD. C57BL/6 mice were treated with PBS (Control), 4.25% glucose PDS for 8 weeks (PDS), or 1 mg/kg rapamycin plus 4.25% glucose PDS for later time points (weeks 5-8) for a total of 4 weeks (PDS plus Rapa). A. H&E staining and Masson's trichrome staining of parietal peritoneum (original magnification $\times 200$). B. The function of peritoneal permeability checked by PET-glucose. C. The function of peritoneal permeability checked by PET-BUN analysis. The results represent the mean \pm SD of five mice in each group. Key: (*) $P < 0.05$ vs. control, (#) $P < 0.05$ vs. PDS group.

0.683, $P = 0.042$), and between the data from filipin staining and the protein expression levels of α -SMA ($r = 0.871$, $P = 0.002$) and collagen I ($r = 0.793$, $P = 0.011$). The data suggest that the preventive effect of rapamycin against PF could be closely associated with the decrease in lipid accumulation.

Rapamycin inhibits ECM deposition and lipid accumulation induced by high-glucose PDS in HPMCs

Consistent with the results from *in vivo* experiments, exposure of HPMCs to high-glucose PDS increased mRNA and protein expression levels of ECM markers α -SMA and collagen I. Co-treatment with rapamycin demonstrated amelioration of high-glucose PDS-induced ch-

anges in ECM components (**Figure 5A-C**). We also examined the inhibitory effect of rapamycin on intracellular lipid content via HPLC assay. As shown in **Figure 5D**, high-glucose PDS stimulation markedly elevated the lipid content in HPMCs. Treatment with rapamycin significantly abrogated the PDS-induced intracellular lipid accumulation.

Rapamycin restores intracellular lipid homeostasis after high-glucose PDS in HPMCs

Because intracellular lipid homeostasis is controlled by lipid influx and efflux mechanisms, we further investigated the effect of rapamycin on LDLr-mediated intracellular cholesterol influx and ABCA1-mediated intracellular cholesterol efflux in HPMCs. We demonstrated that HPMCs

Rapamycin-induced inhibition of peritoneal fibrosis

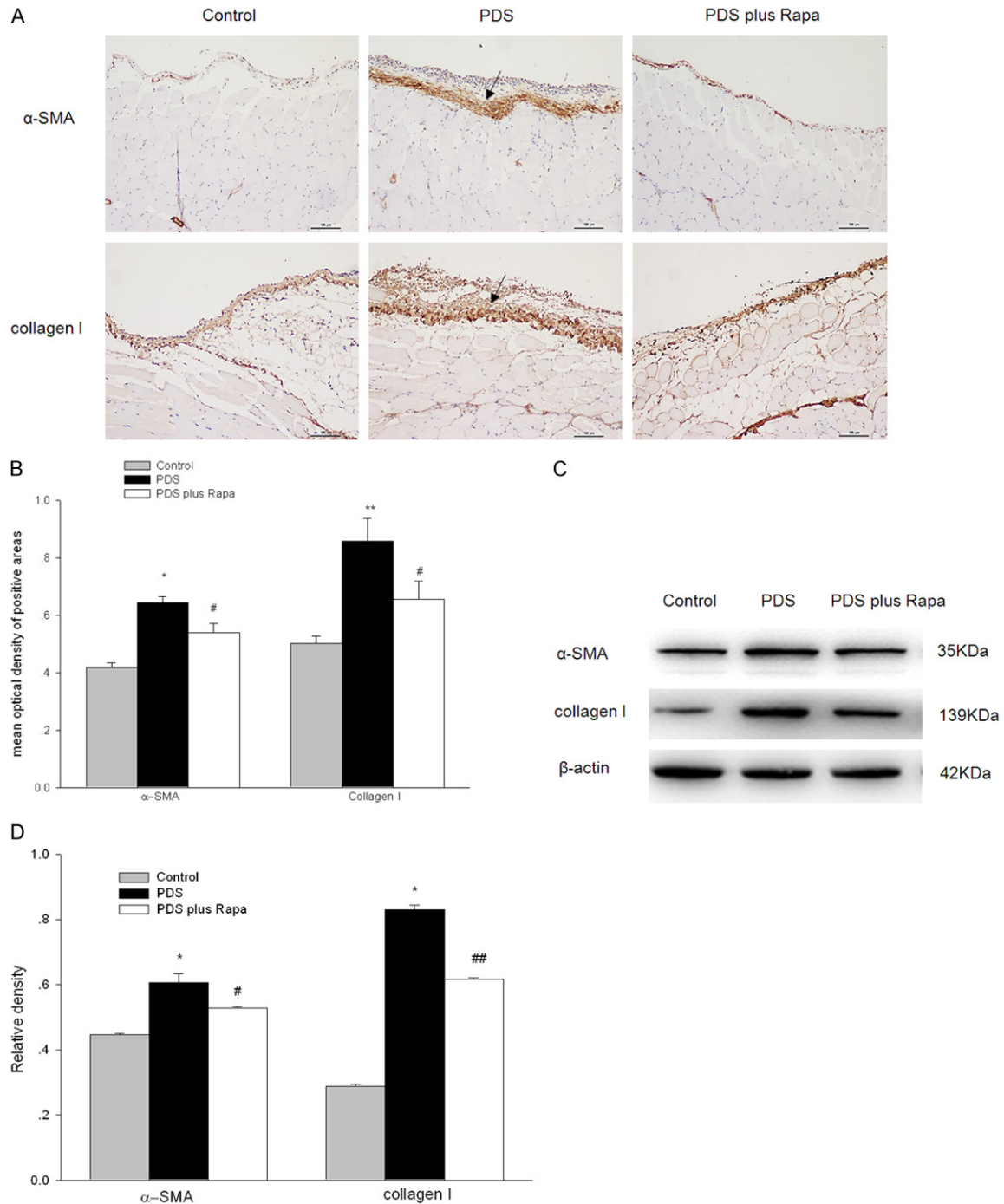


Figure 2. Rapamycin prevented α -SMA and collagen I deposition in the parietal peritoneum in a mouse model of PD. C57BL/6 mice treated with PBS (Control), 4.25% glucose PDS for 8 weeks (PDS), or 1 mg/kg rapamycin plus 4.25% glucose PDS for later time points (weeks 5-8) for a total of 4 weeks (PDS plus Rapa). A. Immunohistochemistry staining of α -SMA and collagen I in the area of parietal peritoneum. The positive areas were stained brown (original magnification $\times 200$). B. The values of semiquantitative analysis for the positive areas were expressed as the mean \pm SD from five mice in each group. Key: (*) $P < 0.05$ vs. control, (**) $P < 0.01$ vs. control, (#) $P < 0.05$ vs. PDS group. C and D. The protein levels of α -SMA and collagen I of visceral peritoneum were further determined by western blot analyses. Identical total protein concentrations extracted from peritoneal tissues were resolved by gel electrophoresis and transferred onto polyvinylidene difluoride membranes. The membranes were subjected to western blotting using anti-mouse polyclonal antibodies against α -SMA, collagen I, or β -actin, which was used as an internal control. The histogram shows the mean \pm SD of the densitometric scans of the protein bands from five mice following normalization by comparison with β -actin. Key: (*) $P < 0.05$ vs. control, (#) $P < 0.05$ vs. PDS group, (##) $P < 0.001$ vs. PDS group.

Rapamycin-induced inhibition of peritoneal fibrosis

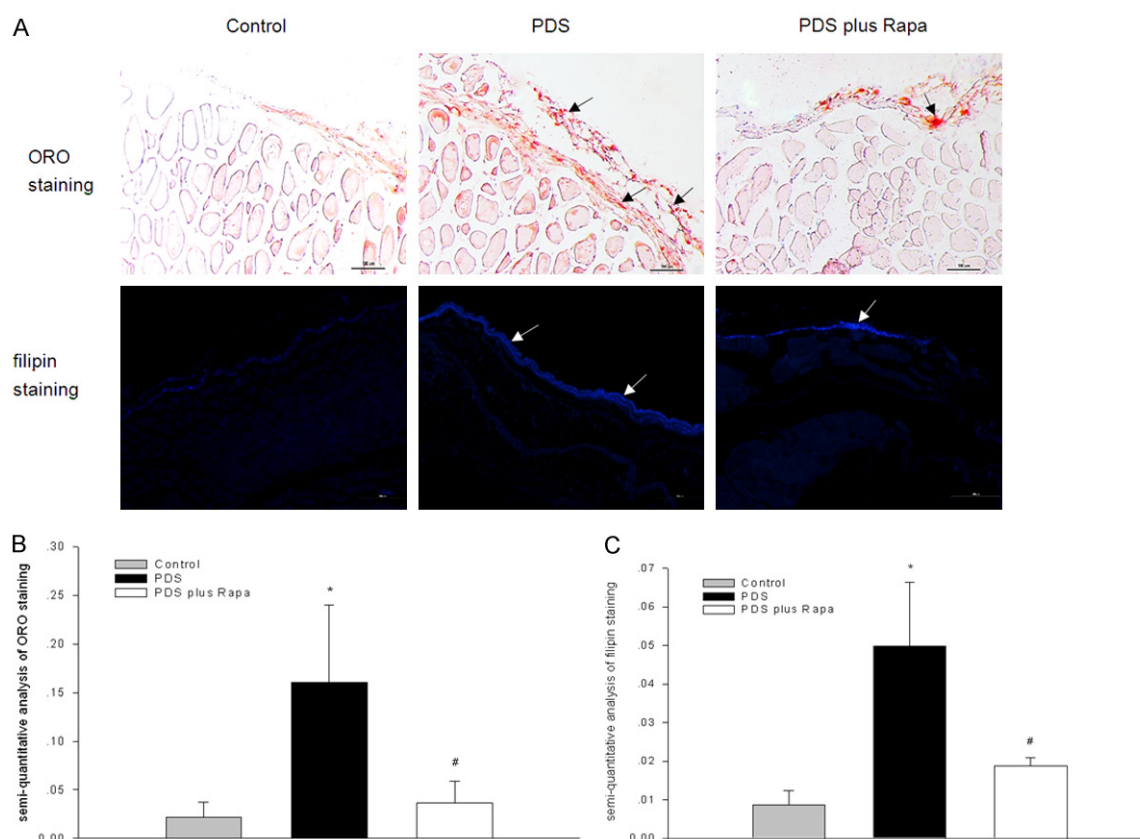


Figure 3. Rapamycin prevented lipid accumulation in the parietal peritoneum in a mouse model of PD. C57BL/6 mice treated with PBS (Control), 4.25% glucose PDS for 8 weeks (PDS), or 1 mg/kg rapamycin plus 4.25% glucose PDS for later time points (weeks 5-8) for a total of 4 weeks (PDS plus Rapa). A. Lipid accumulation in the parietal peritoneum observed by ORO and filipin staining (original magnification $\times 200$). B. The values of semi-quantitative analysis for the positive areas of ORO staining (red color) are expressed as the mean \pm SD from five mice in each group. Key: (*) $P < 0.05$ vs. control, (#) $P < 0.05$ vs. PDS group. C. The values of semi-quantitative analysis for the positive areas of filipin staining (blue color) are expressed as the mean \pm SD from five mice in each group. (*) $P < 0.05$ vs. control, (#) $P < 0.05$ vs. PDS group.

under high-glucose-PDS conditions exhibited increased mRNA and protein levels of LDLr, SREBP-2, and SCAP (Figure 6A-C). In addition, high-glucose-PDS conditions significantly decreased mRNA and protein levels of ABCA1, LXR α , and PPAR α (Figure 6D-F). Treatment with rapamycin significantly abrogated the high-glucose PDS-stimulated activities of these proteins *in vitro* in HPMCs. Taken together, these data suggest that lipid accumulation due to high-glucose PDS conditions in HPMCs was caused by disruption of intracellular lipid influx and efflux mechanisms, and rapamycin restored intracellular lipid homeostasis.

Discussion

PD-induced PF is associated with progressive increased thickness of the peritoneal mem-

brane, predominantly in the submesothelial compact collagenous zone, and membrane hyperpermeability [22]. Long-term exposure of the peritoneal membrane to conventional high-glucose concentration PDS and glucose degradation products (GDP) may play an important role in the underlying mechanisms of PD structural and functional changes in the peritoneum; however this topic remains unclear. Unfortunately, effective clinical therapy for PF is scarce [23]. Recently, several articles reported that the anti-fibrotic effect of rapamycin may be useful in the treatment of PF [19, 20, 24, 25] and encapsulating peritoneal sclerosis, which is the most severe form of PF [26, 27]. However, the underlying mechanisms of the protective role of rapamycin against PF have not been thoroughly elucidated to date. In this study, we demonstrated that rapamycin has an obvious

Rapamycin-induced inhibition of peritoneal fibrosis

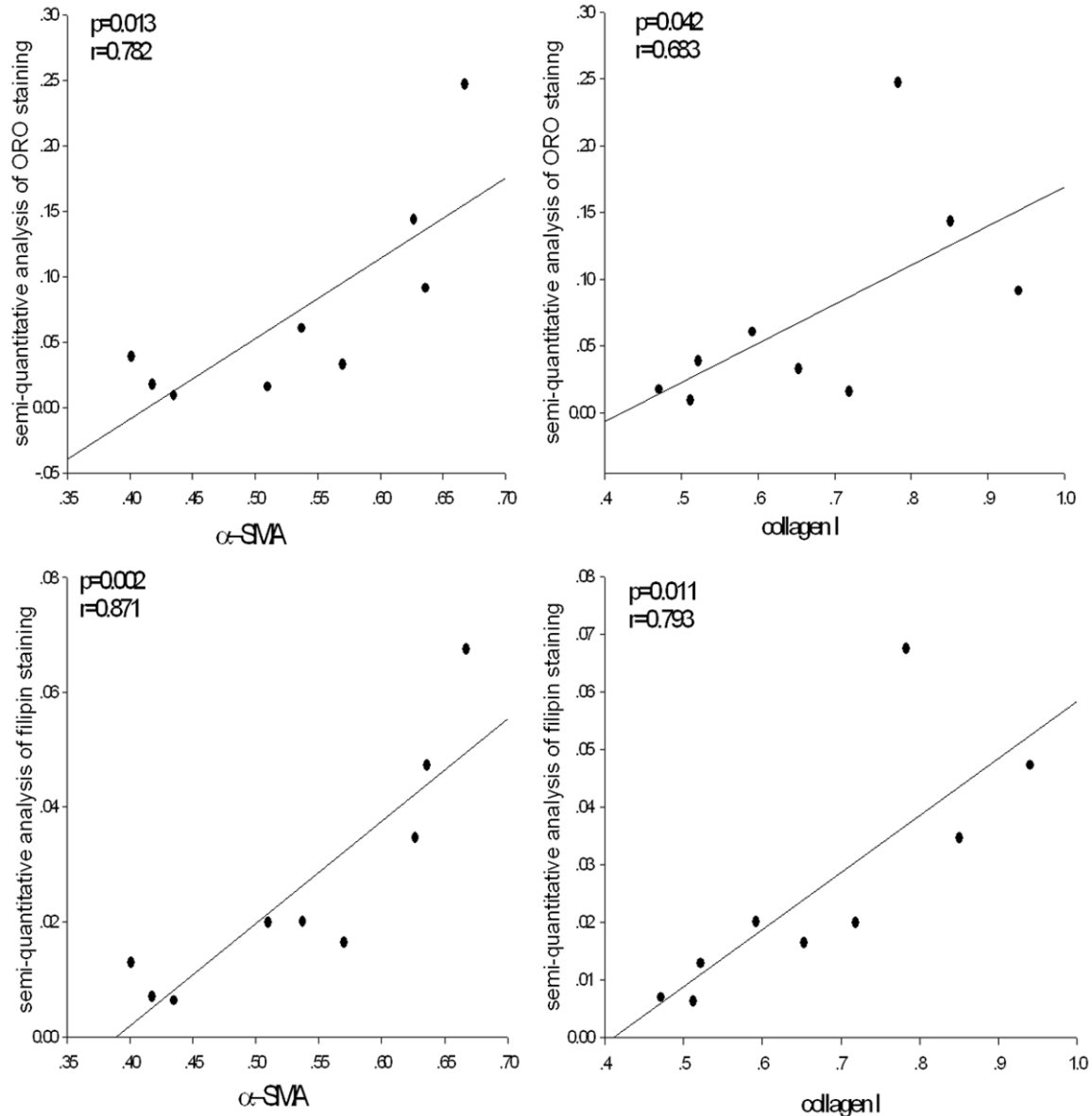


Figure 4. Correlation analysis between lipid and ECM accumulation in the parietal peritoneum in a PD mouse model. C57BL/6 mice treated with PBS (Control), 4.25% glucose PDS for 8 weeks (PDS), or 1 mg/kg rapamycin plus 4.25% glucose PDS for later time points (weeks 5-8) for a total of 4 weeks (PDS plus Rapa). According to data from ORO and filipin staining, lipid droplet accumulation showed a significant positive correlation with α -SMA and collagen I protein levels based on western blot data. The p -values were two-tailed, and $P < 0.05$ was considered significant.

effect on PF inhibition by restoring homeostasis of intracellular lipid influx and efflux mechanisms in the peritoneum under high-glucose-PDS conditions.

A previous study reported that C57BL/6 mice receiving daily intraperitoneal injections of 3 ml 4.25% glucose dialysis solution for 4 weeks manifested typical features of PD, including loss of the mesothelial cell monolayer, thickening of the submesothelial compact zone within

the anterior abdominal wall, and increased peritoneal permeability, thereby confirming the successful establishment of a PF mouse model [21]. We employed the same animal model, and data shown in **Figures 1** and **2** provide evidence that the mice that received high-glucose PDS infusions exhibited typical characteristics of PF, including markedly increased peritoneal thickness, excessive ECM deposition, enhanced peritoneal permeability, as well as higher expression levels of ECM components, such as

Rapamycin-induced inhibition of peritoneal fibrosis

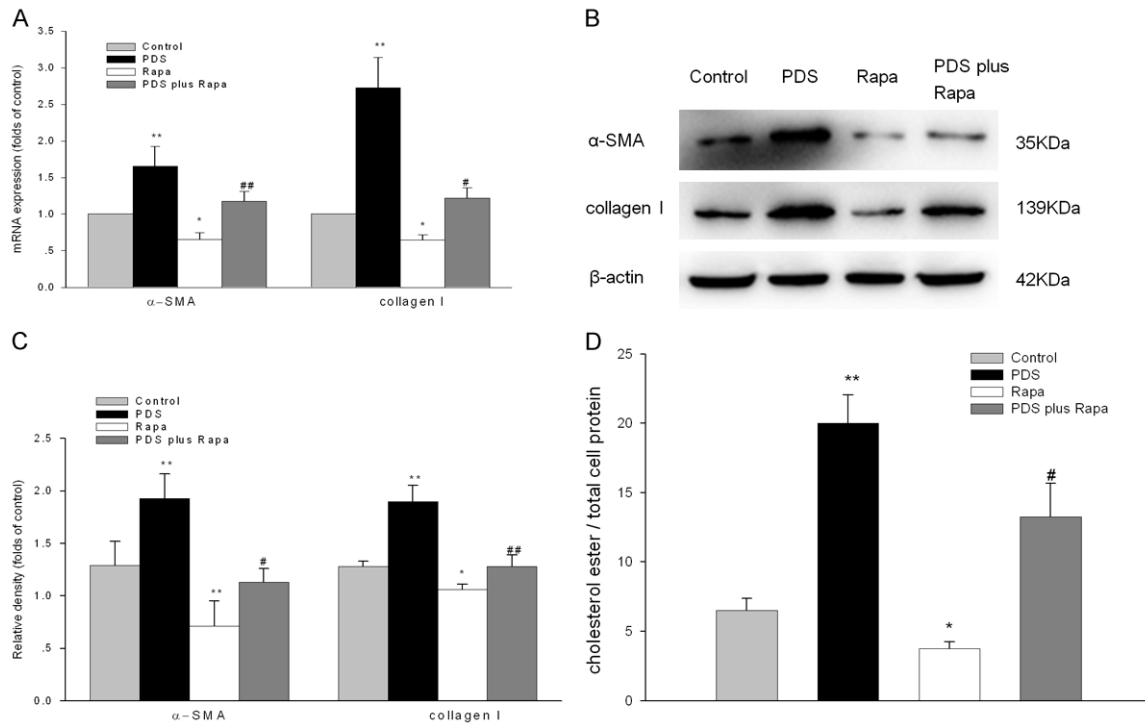


Figure 5. Rapamycin inhibited ECM deposition and lipid accumulation activated by high-glucose PDS in HPMCs. HPMCs were untreated (Control) or treated with 4.25% glucose PDS (PDS), or 10 ng/ml of rapamycin (Rapa), or 4.25% glucose PDS+10 ng/ml of rapamycin (PDS plus Rapa) for 24 h. A. The mRNA expression of α -SMA and collagen I was determined by RT-PCR. Total RNA was extracted from HPMCs, and cDNA was acquired by reverse transcription. β -Actin served as the housekeeping gene. The results represent the mean \pm SD from three experiments. Key: (*) $P < 0.05$ vs. control, (**) $P < 0.001$ vs. control, (#) $P < 0.05$ vs. PDS group, (##) $P < 0.01$ vs. PDS group. B and C. The protein levels of α -SMA and collagen I were examined by western blot analyses. Identical total protein concentrations from HPMCs were resolved by gel electrophoresis and transferred onto polyvinylidene difluoride membranes. The membranes were subjected to western blot analysis using anti-human polyclonal antibodies against α -SMA, collagen I, or β -actin, which was used as an internal control. The histogram represents the mean \pm SD of the densitometric scans for protein bands from three experiments normalized by comparison with β -actin. Key: (*) $P < 0.05$ vs. control, (**) $P < 0.01$ vs. control, (#) $P < 0.01$ vs. PDS group, (##) $P < 0.001$ vs. PDS group. D. The concentration of cholesterol ester in HPMCs was measured using the HPLC assay described in the Materials and Methods section. Values are the mean \pm SD of triplicate wells from three experiments. Key: (*) $P < 0.05$ vs. control, (**) $P < 0.001$ vs. control, (#) $P < 0.001$ vs. PDS group.

α -SMA and collagen I. However, rapamycin notably relieved the characteristics of PF and improved peritoneal function, resulting in decreased peritoneal thickness, reduced collagen deposits, decreased peritoneal permeability, and inhibition of α -SMA and collagen I expression levels. The underlying molecular basis of the protective role of rapamycin against high-glucose PDS-induced PF is not clear. Xiang *et al.* showed that rapamycin notably improved peritoneal function and relieved the signs of high-glucose-induced PF, including reversal of epithelial to mesenchymal transition of the peritoneal mesothelium, as a result of inhibition of Rho GTPase activation [19]. Tamer *et al.* also demonstrated that rapamycin may be ben-

eficial in preventing or delaying the progression of PF and neoangiogenesis. These alterations in the peritoneal membrane may be connected with reduced tumor necrosis factor- α and transforming growth factor- β (TGF- β) levels [28]. In this study, we observed that high-glucose PDS conditions clearly increased lipid deposition both *in vivo* and *in vitro*, and rapamycin reversed the phenomenon. Moreover, there was a parallel decrease in intracellular cholesterol deposition and protein expression levels of α -SMA and collagen I with rapamycin treatment. The data suggest that the preventive effect of rapamycin against PF could be closely associated with decreased lipid accumulation in the peritoneum.

Rapamycin-induced inhibition of peritoneal fibrosis

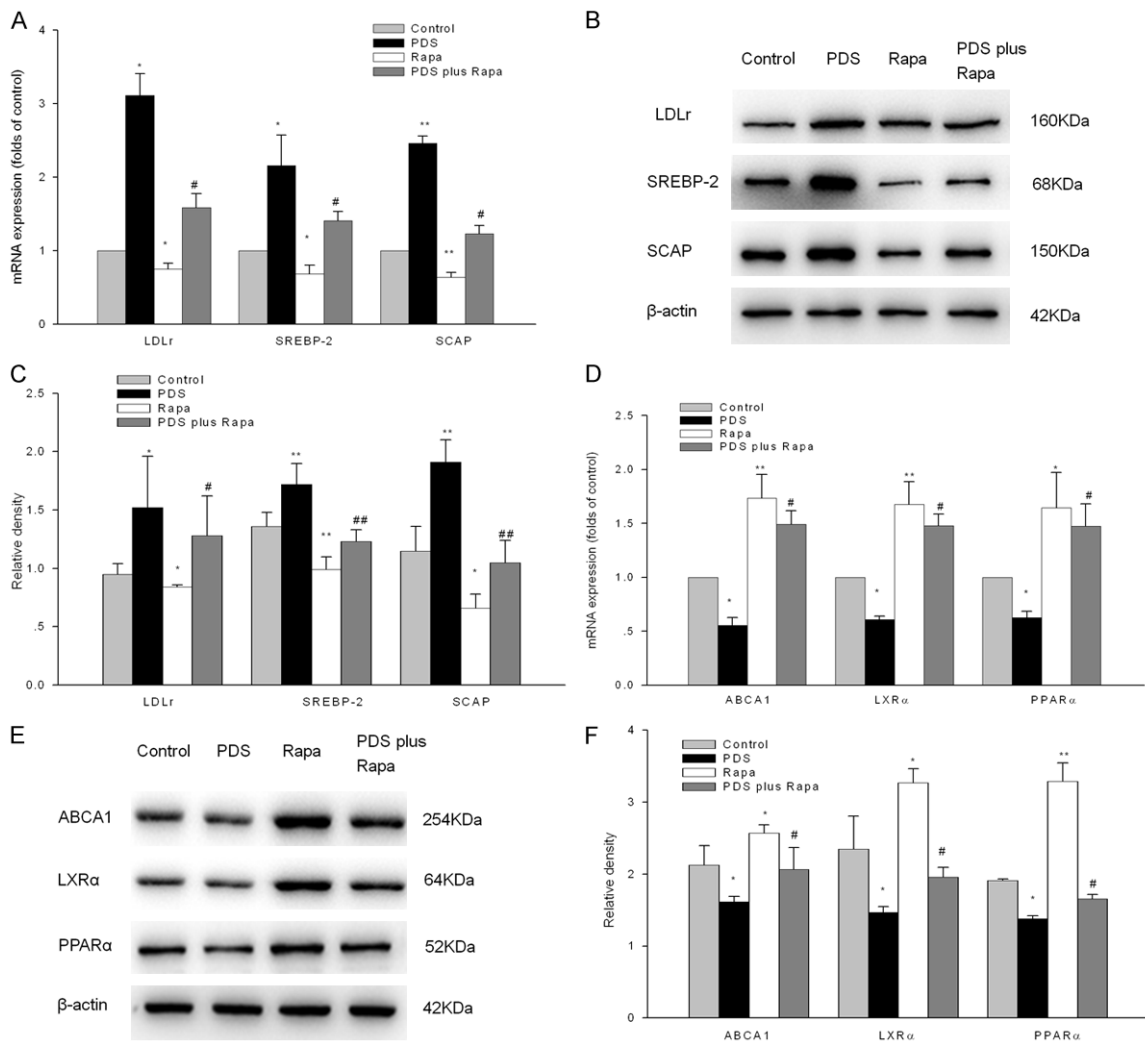


Figure 6. Rapamycin decreased the LDLr-mediated lipid influx, and increased ABCA1-mediated lipid efflux induced by high-glucose PDS in HPMCs. HPMCs were treated without (Control) or with 4.25% glucose PDS (PDS), or 10 ng/ml of rapamycin (Rapa), or 4.25% glucose PDS+10 ng/ml of rapamycin (PDS plus Rapa) for 24 h. A. The mRNA expression levels of LDLr, SREBP-2, and SCAP was determined by RT-PCR. Total RNA was extracted from HPMCs, and cDNA was acquired by reverse transcription. β -Actin served as the housekeeping gene. The results represent the mean \pm SD from three experiments. Key: (*) $P < 0.05$ vs. control, (**) $P < 0.001$ vs. control, (#) $P < 0.05$ vs. PDS group. B and C. The protein levels of LDLr, SREBP-2, and SCAP were examined by western blotting. The identical total protein extracted from HPMCs was isolated by gel electrophoresis and transferred onto polyvinylidene difluoride membranes. The membranes were subjected to western blot analyses using anti-human polyclonal antibodies against LDLr, SREBP-2, SCAP, or β -actin, which was used as an internal control. The histogram represents the mean \pm SD of the densitometric scans for protein bands from three experiments, normalized to β -actin protein levels. Key: (*) $P < 0.05$ vs. control, (**) $P < 0.01$ vs. control, (#) $P < 0.05$ vs. PDS group, (##) $P < 0.001$ vs. PDS group. D. The mRNA expression levels of ABCA1, LXR α , and PPAR α were determined by RT-PCR. Total RNA was extracted from HPMCs, and cDNA was acquired by reverse transcription. β -Actin served as the housekeeping gene. The results represent the mean \pm SD from three experiments. Key: (*) $P < 0.01$ vs. control, (**) $P < 0.001$ vs. control, (#) $P < 0.01$ vs. PDS group. E and F. The protein levels of ABCA1, LXR α , and PPAR α were examined by western blot analysis. Identical total protein concentrations extracted from HPMCs were resolved by gel electrophoresis and transferred onto polyvinylidene difluoride membranes. The membranes were subjected to western blot analyses using anti-human polyclonal antibodies against ABCA1, LXR α , PPAR α , or β -actin, which was used as an internal control. The histogram represents the mean \pm SD of the densitometric scans for protein bands from three experiments, normalized to β -actin levels. Key: (*) $P < 0.05$ vs. control, (**) $P < 0.01$ vs. control, (#) $P < 0.05$ vs. PDS group.

To further delineate potential regulatory mechanisms between rapamycin and lipid metabo-

lism in the peritoneum in response to high-glucose PDS conditions, we targeted detection of

Rapamycin-induced inhibition of peritoneal fibrosis

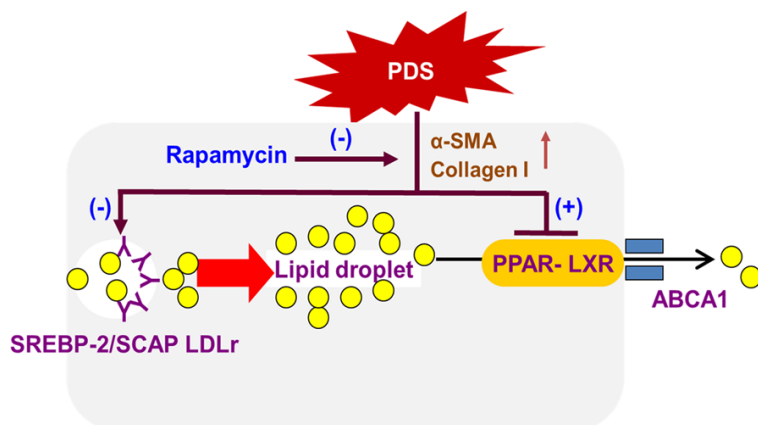


Figure 7. Schematic representation of the outlined hypothesis. High-glucose PDS upregulated the expression of α -SMA and collagen I, and rapamycin significantly inhibited high-glucose PDS-induced ECM accumulation in the peritoneum, which manifested as decreased expression levels of α -SMA and collagen I. These effects correlated with a decrease in the LDLr-mediated lipid influx mechanism, which was mediated through downregulation of SREBP-2 and SCAP expression levels, as well as an increase in the ABCA1-mediated lipid efflux pathway, which was mediated through the upregulation of LXR α and PPAR α expression levels. Overall, rapamycin showed an obvious protective effect against high-glucose PDS-induced PF, which was partly due to restoration of lipid homeostasis in PMCs. Abbreviations: α -SMA, alpha-smooth muscle actin; LDLr, low density lipoprotein receptor; SREBP-2, sterol regulatory element-binding protein-2; SCAP, SREBP cleavage activating protein; ABCA1, adenosine triphosphate-binding cassette transporter A1; LXR α , liver X receptor alpha; PPAR α , peroxisome-proliferator activated receptor alpha.

LDLr-mediated intracellular cholesterol influx and ABCA1-mediated intracellular cholesterol efflux mechanisms *in vitro*. Our experiments show that rapamycin prevented lipid accumulation in HPMCs by 1) inhibiting gene expression and protein levels of LDLr, SREBP-2, and SCAP; and 2) upregulating the expression levels of ABCA1, LXR α , and PPAR α , thereby overriding the increased cholesterol influx induced by 4.25% glucose PDS. Recently, Inokuchi-Shimizu *et al.* found that rapamycin successfully restored autophagy and PPAR α function, thereby reducing lipid accumulation in TGF β -activated kinase 1 (Tak1)-deficient livers of mice and in turn preventing spontaneous liver fibrosis and hepatocarcinogenesis [29]. Martinet *et al.* suggested that systemic administration of rapamycin to different animal models of atherosclerosis strongly inhibits atherosclerotic plaque development, potentially by preventing lipid accumulation in atherosclerotic plaques due to stimulation of cholesterol efflux pathways via upregulation of cholesterol efflux genes as well as downregulation of LDL and scavenger receptors genes [30]. Overall, our results were par-

tially consistent with the conclusions of previous research that showed that rapamycin prevented PF by restoring intracellular lipid homeostasis.

In summary, the present study demonstrates that PD-related PF was closely associated with increased accumulation of lipid droplets in the peritoneum. Inhibition of cellular lipid uptake and elevated cholesterol efflux are important aspects for the anti-fibrotic effects of rapamycin on PMCs (Figure 7). These findings suggest that rapamycin treatment may be a promising therapeutic strategy for the preservation of peritoneal membrane integrity in long-term PD patients.

Acknowledgements

This study was supported by grants from the National Natural Science Foundation of

China (No. 81500585), the Nanjing Medical Science and Technique Development Foundation (No. QRX17120), and the Key Project supported by Medical Science and Technology Development Foundation, Nanjing Department of Health (No. YKK18068).

Disclosure of conflict of interest

None.

Address correspondence to: Drs. Miao Zhang and Jing Liu, Institute of Nephrology, Affiliated Drum Tower Hospital, Medical School of Nanjing University, NO. 321, Zhongshan Road, Nanjing 210008, Jiangsu Province, China. Tel: 0086 25 83106666; E-mail: 15062229898@163.com (MZ); lemiliay@163.com (JL)

References

- [1] Mehrotra R, Devuyst O, Davies SJ, Johnson DW. The Current state of peritoneal dialysis. *J Am Soc Nephrol* 2016; 27: 3238-3252.
- [2] Wu J, Xing C, Zhang L, Mao H, Chen X, Liang M, Wang F, Ren H, Cui H, Jiang A, Wang Z, Zou M, Ji Y. Autophagy promotes fibrosis and apopto-

Rapamycin-induced inhibition of peritoneal fibrosis

- sis in the peritoneum during long-term peritoneal dialysis. *J Cell Mol Med* 2018; 22: 1190-1201.
- [3] Wang L, Balzer MS, Rong S, Menne J, von Vietinghoff S, Dong L, Gueler F, Jang MS, Xu G, Timrott K, Tkachuk S, Hiss M, Haller H, Shushakova N. Protein kinase C α inhibition prevents peritoneal damage in a mouse model of chronic peritoneal exposure to high-glucose dialysate. *Kidney Int* 2016; 89: 1253-1267.
- [4] Hu ZB, Ma KL, Zhang Y, Wang GH, Liu L, Lu J, Chen PP, Lu CC, Liu BC. Inflammation-activated CXCL16 pathway contributes to tubulointerstitial injury in mouse diabetic nephropathy. *Acta Pharmacol Sin* 2018; 39: 1022-1033.
- [5] Ma KL, Gong TK, Hu ZB, Zhang Y, Wang GH, Liu L, Chen PP, Lu J, Lu CC, Liu BC. Lipoprotein(a) accelerated the progression of atherosclerosis in patients with end-stage renal disease. *BMC Nephrol* 2018; 19: 192-199.
- [6] Wu Y, Ma KL, Zhang Y, Wen Y, Wang GH, Hu ZB, Liu L, Lu J, Chen PP, Ruan XZ, Liu BC. Lipid disorder and intrahepatic renin-angiotensin system activation synergistically contribute to non-alcoholic fatty liver disease. *Liver Int* 2016; 36: 1525-1534.
- [7] Ma KL, Liu J, Ni J, Zhang Y, Lv LL, Tang RN, Ni HF, Ruan XZ, Liu BC. Inflammatory stress exacerbates the progression of cardiac fibrosis in high-fat-fed apolipoprotein E knockout mice via endothelial-mesenchymal transition. *Int J Med Sci* 2013; 10: 420-426.
- [8] Chang TI, Kang HY, Kim KS, Lee SH, Nam BY, Paeng J, Kim S, Park JT, Yoo TH, Kang SW, Han SH. The effect of statin on epithelial-mesenchymal transition in peritoneal mesothelial cells. *PLoS One* 2014; 9: e109628-109638.
- [9] Ma KL, Ruan XZ, Powis SH, Chen Y, Moorhead JF, Varghese Z. Inflammatory stress exacerbates lipid accumulation in hepatic cells and fatty livers of apolipoprotein E knockout mice. *Hepatology* 2008; 48: 770-781.
- [10] Nohturfft A, DeBose-Boyd RA, Scheek S, Goldstein JL, Brown MS. Sterols regulate cycling of SREBP cleavage-activating protein (SCAP) between endoplasmic reticulum and Golgi. *Proc Natl Acad Sci U S A* 1999; 20: 11235-11240.
- [11] Schmitz G, Langmann T. Transcriptional regulatory networks in lipid metabolism control ABCA1 expression. *Biochim Biophys Acta* 2005; 1735: 1-19.
- [12] Lloberas N, Cruzado JM, Franquesa M, Herrero-Fresneda I, Torras J, Alperovich G, Rama I, Vidal A, Grinyó JM. Mammalian target of rapamycin pathway blockade slows progression of diabetic kidney disease in rats. *J Am Soc Nephrol* 2006; 17: 1395-1404.
- [13] Liu J, Ma KL, Zhang Y, Wu Y, Hu ZB, Lv LL, Tang RN, Liu H, Ruan XZ, Liu BC. Activation of mTORC1 disrupted LDL receptor pathway: a potential new mechanism for the progression of non-alcoholic fatty liver disease. *Int J Biochem Cell Biol* 2015; 61: 8-19.
- [14] Ma KL, Liu J, Wang CX, Ni J, Zhang Y, Wu Y, Lv LL, Ruan XZ, Liu BC. Activation of mTOR modulates SREBP-2 to induce foam cell formation through increased retinoblastoma protein phosphorylation. *Cardiovasc Res* 2013; 100: 450-460.
- [15] Yoshizaki A, Yanaba K, Yoshizaki A, Iwata Y, Komura K, Ogawa F, Takenaka M, Shimizu K, Asano Y, Hasegawa M, Fujimoto M, Sato S. Treatment with rapamycin prevents fibrosis in tight-skin and bleomycin-induced mouse models of systemic sclerosis. *Arthritis Rheum* 2010; 62: 2476-2487.
- [16] Ma KL, Ruan XZ, Powis SH, Moorhead JF, Varghese Z. Anti-atherosclerotic effects of sirolimus on human vascular smooth muscle cells. *Am J Physiol Heart Circ Physiol* 2007; 292: H2721-H2728.
- [17] Yu M, Kang X, Xue H, Yin H. Toll-like receptor 4 is up-regulated by mTOR activation during THP-1 macrophage foam cells formation. *Acta Biochim Biophys Sin (Shanghai)* 2011; 43: 940-947.
- [18] Zhang GJ, Li H, Li XW. Effects of rapamycin on intracellular cholesterol homeostasis of glomerular mesangial cell in the presence of interleukin-1 beta. *Chin Med Sci J* 2008; 23: 205-211.
- [19] Xiang S, Li M, Xie X, Xie Z, Zhou Q, Tian Y, Lin W, Zhang X, Jiang H, Shou Z, Chen J. Rapamycin inhibits epithelial-to-mesenchymal transition of peritoneal mesothelium cells through regulation of Rho GTPases. *FEBS J* 2016; 283: 2309-2325.
- [20] Xu T, Xie JY, Wang WM, Ren H, Chen N. Impact of rapamycin on peritoneal fibrosis and transport function. *Blood Purif* 2012; 34: 48-57.
- [21] Yu JW, Duan WJ, Huang XR, Meng XM, Yu XQ, Lan HY. MicroRNA-29b inhibits peritoneal fibrosis in a mouse model of peritoneal dialysis. *Lab Invest* 2014; 94: 978-990.
- [22] Che M, Shi T, Feng S, Li H, Zhang X, Feng N, Lou W, Dou J, Tang G, Huang C, Xu G, Qian Q, Sun S, He L, Wang H. The microRNA-199a/214 cluster targets E-cadherin and claudin-2 and promotes high glucose-induced peritoneal fibrosis. *J Am Soc Nephrol* 2017; 28: 2459-2471.
- [23] Zhou Q, Bajo MA, Del Peso G, Yu X, Selgas R. Preventing peritoneal membrane fibrosis in peritoneal dialysis patients. *Kidney Int* 2016; 90: 515-524.
- [24] Sekiguchi Y, Zhang J, Patterson S, Liu L, Hamada C, Tomino Y, Margetts PJ. Rapamycin inhibits transforming growth factor β -induced peritoneal angiogenesis by blocking the sec-

Rapamycin-induced inhibition of peritoneal fibrosis

- ondary hypoxic response. *J Cell Mol Med* 2012; 16: 1934-1945.
- [25] González-Mateo GT, Aguirre AR, Loureiro J, Abensur H, Sandoval P, Sánchez-Tomero JA, del Peso G, Jiménez-Heffernan JA, Ruiz-Carpio V, Selgas R, López-Cabrera M, Aguilera A, Liappas G. Rapamycin protects from type-i peritoneal membrane failure inhibiting the angiogenesis, lymphangiogenesis, and Endo-MT. *Biomed Res Int* 2015; 2015: 989560-989574.
- [26] Frascà GM, D'Arezzo M, Ricciatti AM, Balestra E, Taruscia D, Nastasi V, Goteri G. m-TOR inhibitors may be useful in the treatment of encapsulating peritoneal sclerosis (EPS). *J Nephrol* 2014; 27: 587-590.
- [27] Ghadimi M, Dashti-Khavidaki S, Khalili H. mTOR inhibitors for management of encapsulating peritoneal sclerosis: a review of literatures. *Ren Fail* 2016; 38: 1574-1580.
- [28] Sağırođlu T, Sayhan MB, Yađcı MA, Yalta T, Sağırođlu G, opurođlu E, Ođuz S. Comparison of sirolimus and colchicine treatment on the development of peritoneal fibrosis in rats having peritoneal dialysis. *Balkan Med J* 2015; 32: 101-106.
- [29] Inokuchi-Shimizu S, Park EJ, Roh YS, Yang L, Zhang B, Song J, Liang S, Pimienta M, Taniguchi K, Wu X, Asahina K, Lagakos W, Mackey MR, Akira S, Ellisman MH, Sears DD, Olefsky JM, Karin M, Brenner DA, Seki E. TAK1-mediated autophagy and fatty acid oxidation prevent hepatosteatosis and tumorigenesis. *J Clin Invest* 2014; 124: 3566-3578.
- [30] Martinet W, De Loof H, De Meyer GR. mTOR inhibition: a promising strategy for stabilization of atherosclerotic plaques. *Atherosclerosis* 2014; 233: 601-607.